International Journal of Fracture 69: 319–339, 1995.

Elastodynamic stress-intensity factors for a semi-infinite crack under 3-D combined mode loading

LI XIANG PING and LIU CHUN TU
Institute of Mechanics, Academia Sinica, Beijing, 100080, People's Republic of China

Received 9 July 1993; accepted in revised form 17 August 1994

Abstract. The dynamic stress intensity factor histories for a half plane crack in an otherwise unbounded elastic body are analyzed. The crack is subjected to a traction distribution consisting of two pairs of suddenly-applied shear point loads, at a distance L away from the crack tip. The exact expression for the combined mode stress intensity factors as the function of time and position along the crack edge is obtained. The method of solution is based on the direct application of integral transforms together with the Wiener–Hopf technique and the Cagniard–de Hoop method, which were previously believed to be inappropriate. Some features of solutions are discussed and the results are displayed in several figures.

1. Introduction

The elastodynamic transient response of a body containing a crack poses a difficult analytical problem. Both stationary and constantly propagating semi-infinite cracks in a homogeneous, unbounded solid or along the interface of two half-planes have generally been considered. Freund [1], [2] developed important analytical methods to solved the elastodynamic transient problems in a two-dimensional geometric configuration. In recent years, Achenbach and Gautesen [3], [10] investigated elastodynamic steady-state response for a semi-infinite crack under 3-D loading. Freund [4] dealt with the case of incident stress-wave loading, and some extensions have also been considered by Ramirez and Champion [5], [6]. All of these problems possess no fixed characteristic length and hence the solutions exhibit some dynamic similarity. A three-dimensional configuration of particular interest is that of a pair of opposed collinear concentrated loads acting on the crack faces at a fixed distance from the crack edge. Attributed to the existence of the characteristic length in loading, it was long believed that the Wiener–Hopf technique could not be directly applied. Recently, Kuo and Cheng [7], [8] proposed a solution procedure, which directly applies the Wiener–Hopf technique to analyze the elastodynamic fields for crack problems with characteristic lengths in loading in two-dimensional situations. Li and Liu [9] investigated the elastodynamic stress intensity factor histories for three-dimensional elastodynamic crack problems.

In this paper, the dynamic stress intensity factor histories for a half plane crack in an otherwise unbounded elastic body are considered. The crack is subjected to a traction distribution consisting of two pairs of suddenly-applied shear point loads, at a distance L away from the crack tip. The exact expression for the combined mode stress intensity factors as the functions of time and position along the crack edge is obtained. Some features of the solutions are discussed and the results are displayed in several figures.

2. General formulation

In vector notation the Navier equation governing the displacement vector **u** for an isotropic elastic solid is written as

$$\ddot{\mathbf{u}} = C_d^2\nabla(\nabla\cdot\mathbf{u}) - C_s^2\nabla\times(\nabla\times\mathbf{u}), \tag{2.1}$$

where C_d and C_s are the dilatational and shear wave speeds, respectively.

In terms of the Lamé constants λ and μ and the mass density ρ, the wave speeds are given by

$$\left.\begin{aligned} C_d^2 &= \frac{\lambda+2\mu}{\rho} \\ C_s^2 &= \frac{\mu}{\rho} \end{aligned}\right\}. \tag{2.2}$$

It is also useful to introduce the dilatational and shear slownesses a and b, where $a = 1/C_d$ and $b = 1/C_s$. Furthermore, the Rayleigh wave speed of the elastic material is denoted by C_R and its corresponding slowness by c.

A standard approach when solving (2.1) is to introduce the displacement potentials φ and ψ through the Helmholtz decomposition of the displacement vector, i.e.

$$\left.\begin{aligned} &\mathbf{u} = \nabla\varphi + \nabla\times\psi \\ &\nabla\cdot\psi = 0 \end{aligned}\right\}. \tag{2.3}$$

The scalar dilatational wave potential φ and the vector shear wave potential $\psi = (\psi_x, \psi_y, \psi_z)$ satisfy the uncoupled wave equations

$$\left.\begin{aligned} \nabla^2\varphi &= a^2\frac{\partial^2\varphi}{\partial t^2} \\ \nabla^2\psi &= b^2\frac{\partial^2\psi}{\partial t^2} \end{aligned}\right\}. \tag{2.4}$$

The two potentials are coupled through the boundary conditions that characterize the problem to be described.

Consider the elastic body containing a half plane crack depicted in Fig.1. The body is initially stress free and at rest. The material is characterized by the shear modulus μ, the Possion ratio ν, and the mass density ρ. A right-handed rectangular coordinate system is introduced such that the z-axis coincides with the crack edge, and the half plane crack occupies $y = 0$ for $x < 0$. Equal shear traction on the two crack surfaces produces an antisymmetric displacement field. Thus attention can be restricted to the upper half space $y \geqslant 0$. The complete set of boundary conditions to be satisfied by the stress wave fields is:

$$\left.\begin{aligned} &\sigma_{yy}(x,0,z,t) = 0 && -\infty < x < \infty \\ &\sigma_{xy}(x,0,z,t) = P_1\delta(x+L)\delta(z)H(t) && -\infty < x < 0 \\ &\sigma_{yz}(x,0,z,t) = P_2\delta(x+L)\delta(z)H(t) && -\infty < x < 0 \\ &u_x(x,0,z,t) = 0 && 0 < x < \infty \\ &u_z(x,0,z,t) = 0 && 0 < x < \infty \\ &\text{for } -\infty < z < \infty \text{ and } t \geqslant 0 \end{aligned}\right\}. \tag{2.5}$$

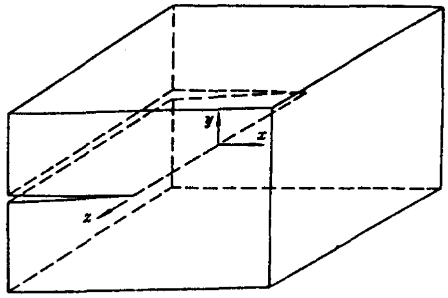

Fig. 1. Geometrical configuration of the elastic solid.

Note that Eqns. (2.5) are defined only on half of the range of x. In order that the two-sided Laplace transform can be applied, the boundary conditions must be extended to apply the full range of x. Thus, the boundary conditions can be rewritten as

$$\left.\begin{aligned} &\sigma_{yy}(x,0,z,t) = 0 \\ &\sigma_{xy}(x,0,z,t) = \sigma_{xy}^{-}(x,z,t) + \sigma_{xy}^{+}(x,z,t) \\ &\sigma_{yz}(x,0,z,t) = \sigma_{yz}^{-}(x,z,t) + \sigma_{yz}^{+}(x,z,t) \\ &u_x(x,0,z,t) = u_x^{-}(x,z,t) \\ &u_z(x,0,z,t) = u_z^{-}(x,z,t) \end{aligned}\right\}, \tag{2.6}$$

for the full range $-\infty < x, z < \infty, 0 < t < \infty$.

Obviously, the superscripts "+" and "−" are used at this point to indicate on which half of the x-axis a superscripted function is nonzero. The notation is carried over into the transformed domain.

The initial conditions are expressed in terms of the displacement potentials by

$$\left.\begin{aligned} &\varphi(x,y,z,0) = 0 \quad \frac{\partial\varphi}{\partial t}(x,y,z,0) = 0 \\ &\psi(x,y,z,0) = 0 \quad \frac{\partial\psi}{\partial t}(x,y,z,0) = 0 \end{aligned}\right\}, \tag{2.7}$$

for $y > 0$. Likewise, the boundary conditions (2.6) can be replaced by their corresponding representations in terms of φ and ψ.

3. Methods of solution

Transform techniques are now used to determine elastodynamic stress intensity factors k_2 and k_3. The following equations are written in terms of the dilatational wave potential φ – the shear wave potential may be treated in a similar manner.

First, the one-sided Laplace transform over time is introduced. The parameter is s, and the transformed function is denoted by a superposed hat. Thus,

$$\hat{\varphi}(x,y,z,s) = \int_0^\infty \varphi(x,y,z,s)\,\mathrm{e}^{-st}\,\mathrm{d}t. \tag{3.1}$$

Next, the dependence on z is suppressed by taking a two-sided Laplace transform with parameter $s\xi$. The transform function is denoted by a superposed bar, i.e.

$$\overline{\hat{\varphi}}(x,y,\xi,s) = \int_{-\infty}^{\infty} \hat{\varphi}(x,y,z,s)\,\mathrm{e}^{-s\xi z}\,\mathrm{d}z. \tag{3.2}$$

Finally, a two-sided Laplace transform over x is taken with parameter $s\eta$. The transformed function is denoted by a capital letter, i.e.

$$\Phi(\eta, y, \xi, s) = \int_{-\infty}^{\infty} \overline{\varphi}(x, y, \xi, s)\,\mathrm{e}^{-s\eta x}\,\mathrm{d}x. \tag{3.3}$$

The governing equations for the potential ϕ and ψ are now transformed, leading to the ordinary differential equations

$$\left.\begin{array}{l} \dfrac{d^2\Phi}{\mathrm{d}y^2} - s^2\alpha^2\Phi = 0 \\ \dfrac{d^2\Psi}{\mathrm{d}y^2} - s^2{\cdot}\beta^2{\cdot}\Psi = 0 \end{array}\right\}, \tag{3.4}$$

where

$$\left.\begin{array}{l} \alpha^2 = a^2 - \eta^2 - \xi^2 \\ \beta^2 = b^2 - \eta^2 - \xi^2 \end{array}\right\}. \tag{3.5}$$

General solutions in the transform domain, which are bounded as $Y \to \infty$, can be written as

$$\left.\begin{array}{l} \Phi(\eta, y, \xi, s) = A\exp(-s\alpha y) \\ \Psi(\eta, y, \xi, s) = B\exp(-s\beta y) \\ B = (B_x, B_y, B_z) \end{array}\right\}. \tag{3.6}$$

The complex η plane is cut along real axis so that $R_e(\alpha) \geqslant 0$ and $R_e(\beta) \geqslant 0$ for each value for ξ. The Laplace transformation of the boundary conditions and (2.3b) provide six equations, i.e:

$$\begin{array}{l} (\beta^2 - \eta^2 - \xi^2)A - 2\xi\beta B_x + 2\eta\beta{\cdot}B_z = 0, \\ -2\eta\alpha A + \xi\eta B_x + \xi\beta B_y + (\beta^2 - \eta^2)B_z = \dfrac{1}{\mu}(\sigma_{xy}^+(\eta, \xi, S) + \sigma_{xy}^-(\eta, \xi, S))/s^2, \\ -(2\xi\alpha A + (\beta^2 - \xi^2)B_x + \eta\beta B_y + \xi\eta B_z) = \dfrac{1}{\mu}(\sigma_{yz}^+ + \sigma_{yz}^-)/s^2, \\ \eta A - \xi B_y - \beta B_z = U_x^-/s, \\ \xi A + \eta B_y + \beta B_x = U_z^-/s, \\ \eta B_x - \beta{\cdot}B_y + \xi B_z = 0, \end{array} \tag{3.7}$$

where

$$\begin{array}{rl} U_x^- &= \displaystyle\int_{-\infty}^{\infty}\int_{-\infty}^{\infty} \hat{u}_x^-(x, z, s)\exp(-s(\xi z + \eta x))\,\mathrm{d}z\,\mathrm{d}x, \\ U_z^- &= \displaystyle\int_{-\infty}^{\infty}\int_{-\infty}^{\infty} \hat{u}_z^-(x, z, s)\exp(-s(\xi z + \eta x))\,\mathrm{d}z\,\mathrm{d}x, \\ \sigma_{xy}^+ &= \displaystyle\int_{-\infty}^{\infty}\int_{-\infty}^{\infty} \hat{\sigma}_{xy}^+(x, z, s)\exp(-s(\xi z + \eta x))\,\mathrm{d}z\,\mathrm{d}x, \\ \sigma_{yz}^+ &= \displaystyle\int_{-\infty}^{\infty}\int_{-\infty}^{\infty} \hat{\sigma}_{yz}^+(x, z, s)\exp(-s(\xi z + \eta x))\,\mathrm{d}z\,\mathrm{d}x. \end{array} \tag{3.8}$$

If A, B_x, B_y, B_z are eliminated from the above equations, two algebraic equations will be obtained

$$\frac{\mu s}{\beta b^2}\begin{bmatrix} E & F \\ F & G \end{bmatrix}\begin{Bmatrix} U_x^- \\ U_z^- \end{Bmatrix} = \begin{Bmatrix} \sigma_{xy}^+ \\ \sigma_{yz}^+ \end{Bmatrix} + \begin{Bmatrix} \sigma_{xy}^- \\ \sigma_{yz}^- \end{Bmatrix}, \tag{3.9}$$

$$\left.\begin{aligned} E &= -4\eta^2\alpha\beta - \eta^2\xi^2 - \beta^2\xi^2 - (\beta^2 - \eta^2)^2 \\ F &= -4\xi\eta\alpha\beta + \eta\xi(\beta^2 - \xi^2) + \eta\xi\beta^2 + \xi\eta(\beta^2 - \eta^2) \\ G &= -4\xi^2\alpha\beta - (\beta^2 - \xi^2)^2 - \eta^2\beta^2 - \eta^2\xi^2 \end{aligned}\right\}. \tag{3.10}$$

In order that the Wiener–Hopf technique can be applied, one hopes the left-matrix can be transformed into a diagonal matrix. After some manipulation, one may obtain

$$\begin{bmatrix} \eta & \xi \\ \xi & -\eta \end{bmatrix}\left\{\begin{pmatrix} \sigma_{xy}^+ \\ \sigma_{yz}^+ \end{pmatrix} + \begin{pmatrix} \sigma_{xy}^- \\ \sigma_{yz}^- \end{pmatrix}\right\} = -\mu s\begin{bmatrix} \frac{R}{\beta b^2} & 0 \\ 0 & \beta \end{bmatrix}\begin{bmatrix} \eta & \xi \\ \xi & -\eta \end{bmatrix}\begin{Bmatrix} U_x^- \\ U_z^- \end{Bmatrix}. \tag{3.11}$$

If we set $\xi = iu$ and u is a real, then the matrix notation is

$$\Sigma^+ + \Sigma^- = -\frac{\mu s}{\eta^2 - u^2}\chi(\eta)D(\eta)\chi(\eta)U^-, \tag{3.12}$$

where

$$R(\eta, u) = (\beta^2 - \eta^2 + u^2)^2 + 4\alpha\beta(\eta^2 - u^2),$$

$$\alpha = \sqrt{a^2 - \eta^2 + u^2}, \quad \beta = \sqrt{b^2 - \eta^2 + u^2},$$

$$\chi(\eta) = \begin{bmatrix} \eta & iu \\ iu & -\eta \end{bmatrix}, \quad D(\eta) = \begin{bmatrix} \dfrac{R(\eta, u)}{\beta b^2} & 0 \\ 0 & \beta \end{bmatrix},$$

$$\Sigma^+ = \begin{pmatrix} \sigma_{xy}^+ \\ \sigma_{yz}^+ \end{pmatrix}, \quad \Sigma^- = \begin{pmatrix} \sigma_{xy}^- \\ \sigma_{yz}^- \end{pmatrix}, \quad U^- = \begin{pmatrix} U_x^- \\ U_z^- \end{pmatrix}. \tag{3.13}$$

Eqns. (3.12) are called Wiener–Hopf equations.

4. Wiener–Hopf technique

Introduce a new function $S(\eta, u)$ by defining

$$S(\eta, u) = \frac{R(\eta, u)}{k(c^2 - \eta^2 + u^2)} \quad k = 2(b^2 - a^2). \tag{4.1}$$

The function $S(\eta, u) \to 1$ as $|\eta| \to \infty$ and it has neither zeros, nor poles in the finite η plane. The only singularities of $S(\eta, u)$ are the branch points at $\eta = \pm\sqrt{a^2 + u^2}$ and at $\eta = \pm\sqrt{b^2 + u^2}$ which are shared with $R(\eta, u)$, and it is single valued in the η–plane cut along $\sqrt{a^2 + u^2} \leqslant |R_e(\eta)| \leqslant \sqrt{b^2 + u^2}$, $I_m(\eta) = 0$. The property that $S(\bar{\eta}, u) = \overline{S(\eta, u)}$ for the restricted range of u may be exploited to show that

$$S_\pm(\eta, u) = \exp\left\{-\frac{1}{\pi}\cdot\int_a^b \tan^{-1}\left(\frac{4\xi^2\sqrt{b^2 - \xi^2}\sqrt{\xi^2 - a^2}}{(b^2 - 2\xi^2)^2}\right)\frac{\xi\, d\xi}{\sqrt{\xi^2 + u^2}(\sqrt{\xi^2 + u^2} \pm \eta)}\right\}, \tag{4.2}$$

where the overbar denotes complex conjugate. The functions $S_+(\eta, u)$ and $S_-(\eta, u)$ are analytic and nonzero in the half planes $R_e(\eta) > -\sqrt{a^2+u^2}$ and $R_e(\eta) < \sqrt{a^2+u^2}$, respectively.

The function β may be factorized as

$$\beta = \sqrt{b^2-\eta^2+u^2} = \left[\sqrt{\sqrt{b^2+u^2}+\eta}\right]_+ \left[\sqrt{\sqrt{b^2+u^2}-\eta}\right]_-, \tag{4.3}$$

thus

$$D(\eta) = D_+(\eta)D_-(\eta). \tag{4.4}$$

Here

$$D_+(\eta) = \begin{bmatrix} \frac{\sqrt{k}}{b}\cdot\frac{(\sqrt{c^2+u^2}+\eta)S_+(\eta,u)}{(\sqrt{b^2+u^2}+\eta)^{1/2}} & 0 \\ 0 & \sqrt{\sqrt{b^2+u^2}+\eta} \end{bmatrix}, \tag{4.5}$$

$$D_-(\eta) = \begin{bmatrix} \frac{\sqrt{k}}{b}\cdot\frac{(\sqrt{c^2+u^2}-\eta)S_-(\eta,u)}{(\sqrt{b^2+u^2}-\eta)^{1/2}} & 0 \\ 0 & \sqrt{\sqrt{b^2+u^2}-\eta} \end{bmatrix}. \tag{4.6}$$

Therefore, (3.10) can be solved to yield in matrix notation

$$\Sigma^+ + \Sigma^- = -\mu s A^+ A^- U^- \tag{4.7}$$

where:

$$\left.\begin{aligned} A^+ &= (\eta+|u|)^{-1}\chi(\eta)D_+(\eta) \\ A^- &= (\eta-|u|)^{-1}D_-(\eta)\chi(\eta) \end{aligned}\right\}. \tag{4.8}$$

To solve (4.7), one first observes that

$$(A^+)^{-1} = (\eta-|u|)^{-1}B^+ \quad B^+ = [D_+(\eta)]^{-1}\chi(\eta), \tag{4.9}$$

and

$$(A^-)^{-1} = (\eta+|u|)^{-1}B^- \quad B^- = \chi(\eta)(D_-(\eta))^{-1}. \tag{4.10}$$

Matrix multiplication of (4.7) by $(A^+)^{-1}$, then gives

$$\begin{aligned} &\frac{1}{s}(\eta-|u|)^{-1}B^+\Sigma^- + \frac{1}{s}(\eta-|u|)^{-1}\{B^+\Sigma^+ - (B^+\Sigma^+)_{\eta=|u|}\} \\ &\quad = -\mu A^- U^- - \frac{1}{s}(\eta-|u|)^{-1}(B^+\Sigma^+)_{\eta=|u|}. \end{aligned} \tag{4.11}$$

One may easily know

$$\begin{aligned} (\eta-|u|)^{-1}B^+\Sigma^- &= \frac{1}{s}\frac{1}{\eta-|u|}\begin{bmatrix} \frac{(\sqrt{b^2+u^2}+\eta)^{1/2}(P_1\eta+iP_2u)}{\sqrt{k}/b(\sqrt{c^2+u^2}+\eta)S_+} \\ \frac{1}{(\sqrt{b^2+u^2}+\eta)^{1/2}}(P_1iu-P_2\eta) \end{bmatrix} e^{s\eta L} \\ &= \frac{1}{s}\frac{G(\eta)}{\eta-|u|} \end{aligned} \tag{4.12}$$

From the above expression one can find that the pole must be removed at $\eta = |u|$, so that

$$\frac{1}{s}\frac{1}{\eta-|u|}\{B^+\Sigma^+ - (B^+\Sigma^+)_{\eta=|u|}\} + \frac{1}{s^2}\frac{1}{\eta-|u|}(G(\eta)-G_0)$$
$$= -\mu A^- U^- - \frac{1}{s}\frac{1}{\eta-|u|}(B^+\Sigma^+)_{\eta=|u|} - \frac{1}{s^2}\frac{G_0}{\eta-|u|}. \tag{4.13}$$

Here

$$G_0 = G(\eta)|_{\eta=|u|}. \tag{4.14}$$

Since the function $(G(\eta)-G_0)/(\eta-|u|)$ is analytic and goes to zero as $|\eta|\to\infty$ in the strip $-\sqrt{b^2+u^2} < R_e(\eta) < \sqrt{b^2+u^2}$, it can be expressed as the sum of the two functions $G_+(\eta)$ and $G_-(\eta)$.

$$\left.\begin{aligned} G_+(\eta) &= -\frac{1}{2\pi i}\int_{Br}\frac{G(Z)-G_0}{Z-|u|}\frac{\mathrm{d}Z}{Z-\eta} \\ G_-(\eta) &= (G(\eta)-G_0)/(\eta-|u|) - G_+(\eta) \end{aligned}\right\}. \tag{4.15}$$

Substituting for $G_+(\eta), G_-(\eta)$ in (4.13), one obtains

$$\frac{1}{s}\frac{1}{\eta-|u|}\{B^+\Sigma^+ - (B^+\Sigma^+)_{\eta=|u|}\} + \frac{1}{s^2}G_+(\eta)$$
$$= -\mu A^- U^- - \frac{1}{s}\frac{1}{\eta-|u|}(B^+\Sigma^+)_{\eta=|u|} - \frac{1}{s^2}\frac{G_0}{\eta-|u|} - \frac{1}{s^2}G_-(\eta). \tag{4.16}$$

The left-hand and right-hand sides of (4.16) are clearly regular in the overlapping half planes $R_e(\eta) < |u|$ and $R_e(\eta) > -\sqrt{b^2+u^2}$, respectively. Consequently, by analytic continuation, both sides represent one and the same entire function $E(\eta)$. According to Liouville's theorem, a bounded entire function is a constant. After some analysis one gets $E(\eta)\equiv 0$. Hence:

$$\begin{aligned} \frac{1}{s}\frac{1}{\eta-|u|}(B^+\Sigma^+) &= \frac{1}{s^2}\left(\frac{s}{\eta-|u|}(B^+\Sigma^+)_{\eta=|u|} - G_+(\eta)\right), \\ -\mu A^- U^- &= \frac{1}{s^2}\left(\frac{s}{\eta-|u|}(B^+\Sigma^+)_{\eta=|u|} + \frac{G_0}{\eta-|u|} + G_-(\eta)\right). \end{aligned} \tag{4.17}$$

The one remaining unknown quantity $B^+\Sigma^+$ at $\eta = |u|$, follows from the requirement that the pole must be removed at $\eta = -|u|$ in order that U^- is analytic in the left-half plane, i.e.

$$\begin{aligned} -\mu U^- &= \frac{1}{s^2}\frac{1}{\eta+|u|}B^-\left[\frac{s}{\eta-|u|}(B^+\Sigma^+)_{\eta=|u|} + \beta^+\right], \\ \beta^+ &= \frac{G_0}{\eta-|u|} + G_-(\eta). \end{aligned} \tag{4.18}$$

After a careful analysis of the right hand side of (4.18), one may find the determinant of the matrix $\chi(\eta)$, defined by (3.13), vanishes at $\eta = \pm|u|$ and consequently $\chi(\eta)$ has rank 1 at that point.

As a consequence B^+, defined by (4.9), also has rank 1 at $\eta = |u|$, and maps all vectors into a vector proportional to

$$\mathbf{e}_1 = (D_2, iD_1 \operatorname{sgn}(u)).$$

Hence, $B^+\Sigma^+$ at $\eta = |u|$ can be expressed as

$$(B^+\Sigma^+)_{\eta=|u|} = g\mathbf{e}_1,$$

where g is a constant which involves linear combinations of the value of Σ^+ at $\eta = |u|$. The constant g must now, however, be chosen such that the residue from the pole is zero. That this is possible follows from the observation that at $\eta = -|u|$ the matrix B^- is singular and maps the vector $\mathbf{e}_1$ into the zero vector. In particular, we have

$$(-D_2, iD_1 \operatorname{sgn}(u)) \left\langle \begin{pmatrix} D_2 \\ iD_1 \operatorname{sgn}(u) \end{pmatrix} \frac{sg}{-2|u|} + (\beta^+)_{\eta=-|u|} \right\rangle = 0,$$

$$sg = 2|u| \frac{\mathbf{e}_2 \cdot (\beta^+)_{\eta=-|u|}}{\mathbf{e}_1 \cdot \mathbf{e}_2}$$

from the above expression and one can find that

$$s(B^+\Sigma^+)_{\eta=|u|} = 2|u| \frac{\mathbf{e}_1}{\mathbf{e}_1 \cdot \mathbf{e}_2} \mathbf{e}_2 \cdot (\beta^+)_{\eta=-|u|}, \tag{4.19}$$

where

$$\left. \begin{aligned} \mathbf{e}_1 &= (D_2, iD_1 \operatorname{sgn}(u)) \\ \mathbf{e}_2 &= (-D_2, iD_1 \operatorname{sgn}(u)) \\ D_2 &= (\sqrt{b^2 + u^2} + |u|)^{1/2} \\ D_1 &= \frac{\sqrt{k}}{b} \cdot \frac{(\sqrt{c^2 + u^2} + |u|) S_+(|u|, u)}{(\sqrt{b^2 + u^2} + |u|)^{1/2}} \end{aligned} \right\}, \tag{4.20}$$

therefore

$$\begin{aligned} \Sigma^+ &= \frac{1}{s} A^+ \left(\frac{2|u|}{\eta - |u|} \frac{\mathbf{e}_1}{\mathbf{e}_1 \cdot \mathbf{e}_2} \mathbf{e}_2 \cdot (\beta^+)_{\eta=-|u|} - G_+(\eta) \right), \\ U^- &= -\frac{1}{\mu s^2} \frac{B^-}{\eta + |u|} \left(\frac{2|u|}{\eta - |u|} \frac{\mathbf{e}_1}{\mathbf{e}_1 \cdot \mathbf{e}_2} \mathbf{e}_2 \cdot (\beta^+)_{\eta=-|u|} + \beta^+ \right). \end{aligned} \tag{4.21}$$

5. The stress intensity factor histories along the edge

Stress intensity factors k_2 and k_3 can now be concluded. It is expected that

$$\left. \begin{aligned} \sigma_{xy}(x, o, z, t) &\sim \frac{k_2(z, t)}{\sqrt{2\pi x}} \\ \sigma_{yz}(x, o, z, t) &\sim \frac{k_3(z, t)}{\sqrt{2\pi x}} \end{aligned} \right. \quad x \to 0^+. \tag{5.1}$$

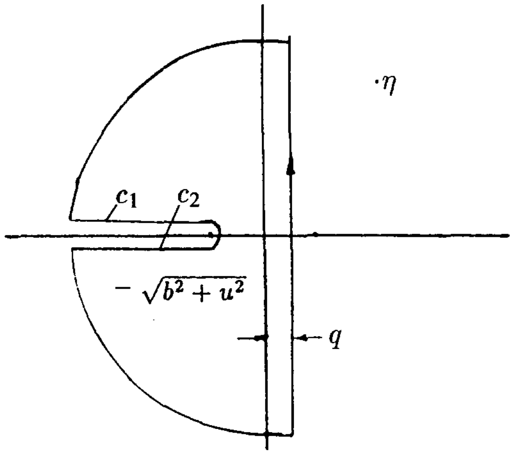

Fig. 2. The integration Bromwich path.

The transformed stress intensity factors may be written as

$$\begin{aligned}\bar{\hat{k}}_2(u,s) &= \lim_{x\to 0+}\Big((2\pi x)^{1/2}\bar{\hat{\sigma}}_{xy}(x,o,u,s)\Big),\\ \bar{\hat{k}}_3(u,s) &= \lim_{x\to 0+}\Big((2\pi x)^{1/2}\bar{\hat{\sigma}}_{yz}(x,o,u,s)\Big).\end{aligned} \tag{5.2}$$

Use of Abel's theorem on the asymptotic properties of the transformed gives

$$\begin{aligned}\bar{\hat{k}}_2(u,s) &= \lim_{\eta\to\infty}\Big((2s\eta)^{1/2}\sigma^{+}_{xy}(\eta,o,u,s)\Big),\\ \bar{\hat{k}}_3(u,s) &= \lim_{\eta\to\infty}\Big((2s\eta)^{1/2}\sigma^{+}_{yz}(\eta,o,u,s)\Big).\end{aligned} \tag{5.3}$$

Therefore

$$\begin{pmatrix}\bar{\hat{k}}_2(u,s)\\ \bar{\hat{k}}_3(u,s)\end{pmatrix} = \lim_{\eta\to\infty}((2s\eta)^{1/2}\Sigma^{+}) = \sqrt{\frac{2}{s}}\begin{bmatrix}\sqrt{k}/b & 0\\ 0 & -1\end{bmatrix}$$

$$\left\langle 2|u|\frac{\mathbf{e}_1}{\mathbf{e}_1\cdot\mathbf{e}_2}\mathbf{e}_2\left\{\frac{1}{2\pi_i}\int_{B_r}\frac{G(z)-G_0}{Z^2-u^2}dZ\right\} - \frac{1}{2\pi i}\int_{B_r}\frac{G(z)-G_0}{Z-|u|}\,\mathrm{d}Z\right\rangle \tag{5.4}$$

After some analysis (see the Appendix), setting $t=\sqrt{b^2+u^2}w$, one obtain

$$\begin{aligned}\bar{\hat{k}}_2 =\; & \frac{1}{\pi}\sqrt{\frac{2}{s}}\Bigg\langle\frac{2|u|(\sqrt{b^2+u^2}+|u|)^2}{(\sqrt{b^2+u^2}+|u|)^2+\frac{k}{b^2}(\sqrt{b^2+u^2}+|u|)^2S_{+}^2}\\ & \times\int_1^{\infty}\frac{\mathrm{e}^{-sL\sqrt{b^2+u^2}w}\,\mathrm{d}w}{(b^2+u^2)w^2-u^2}\frac{\sqrt[4]{b^2+u^2}}{\sqrt{\frac{c^2+u^2}{b^2+u^2}}-w}\frac{(P_1\sqrt{b^2+u^2}w-iP_2u)}{S_{-}(\sqrt{b^2+u^2}w,u)}\\ & \cdot\sqrt{w-1}-\frac{2ui\cdot k}{b^2}\frac{(\sqrt{b^2+u^2}+|u|)(\sqrt{c^2+u^2}+|u|)S_{+}(|u|)}{(\sqrt{b^2+u^2}+|u|)^2+\frac{k}{b^2}(\sqrt{b^2+u^2}+|u|)^2S_{+}^2}\\ & \times\int_1^{\infty}\frac{\sqrt[4]{b^2+u^2}}{(b^2+u^2)w^2-u^2}\frac{P_1iu+P_2\sqrt{b^2+u^2}w}{\sqrt{w-1}}\mathrm{e}^{-sL\sqrt{b^2+u^2}w}\,\mathrm{d}w\end{aligned}$$

$$+\int_1^\infty \frac{\sqrt[4]{b^2+u^2}(P_1\sqrt{b^2+u^2}w - iP_2u)}{(\sqrt{b^2+u^2}w+|u|)} \times \frac{(w-1)^{1/2}\cdot \mathrm{e}^{-sL\cdot\sqrt{b^2+u^2}w}}{\left(\sqrt{\frac{c^2+u^2}{b^2+u^2}}-w\right) S_-(\sqrt{b^2+u^2}w)} \mathrm{d}w \Bigg\rangle, \tag{5.5}$$

$$\begin{aligned}\bar{\hat{k}}_3 = {} & \frac{1}{\pi}\sqrt{\frac{2}{s}}\Bigg\langle \frac{-2ui(\sqrt{b^2+u^2}+|u|)(\sqrt{c^2+u^2}+|u|)S_+(|u|)}{(\sqrt{b^2+u^2}+|u|)^2+\frac{k}{b^2}(\sqrt{c^2+u^2}+|u|)^2 S_+^2} \\ & \times \int_1^\infty \frac{\sqrt[4]{b^2+u^2}(w-1)^{1/2}}{\left(\sqrt{\frac{c^2+u^2}{b^2+u^2}}-w\right)} \frac{(P_1\sqrt{b^2+u^2}w - iP_2u)}{S_-(\sqrt{b^2+u^2}w)((b^2+u^2)w^2-u^2)} \\ & \times \mathrm{e}^{-sL\sqrt{b^2+u^2}w}\,\mathrm{d}w - \frac{2k|u|}{b^2}\frac{(\sqrt{c^2+u^2}+|u|)^2 S_+^2(|u|)}{(\sqrt{b^2+u^2}+|u|)^2+\frac{k}{b^2}(\sqrt{c^2+u^2}+|u|)^2 S_+^2} \\ & \times \int_1^\infty \frac{\sqrt[4]{b^2+u^2}}{(b^2+u^2)w^2-u^2} \frac{P_1 iu + P_2\sqrt{b^2+u^2}w}{\sqrt{w-1}}\mathrm{e}^{-sL\sqrt{b^2+u^2}w} \\ & - \int_1^\infty \frac{\sqrt[4]{b^2+u^2}}{\sqrt{b^2+u^2}w+|u|} \frac{P_1 iu + P_2\sqrt{b^2+u^2}w}{\sqrt{w-1}}\mathrm{e}^{-sL\sqrt{b^2+u^2}w}\,\mathrm{d}w \Bigg\rangle \end{aligned} \tag{5.6}$$

After relaxing the constraint that u is real, inversion of Laplace transform over z gives

$$\begin{pmatrix} \hat{k}_2(z,s) \\ \hat{k}_3(z,s) \end{pmatrix} = \frac{s}{2\pi}\int_{-\infty+u_0 i}^{\infty+u_0 i} \begin{pmatrix} \bar{\hat{k}}_2(u,s) \\ \bar{\hat{k}}_3(u,s) \end{pmatrix} \exp(isuz)\,\mathrm{d}u, \tag{5.7}$$

where $u_0 \in (-b, b)$.

Changing the order of integration between the integrals over the transformed variable u and w, one obtains

$$\begin{pmatrix} \hat{k}_2(z,s) \\ \hat{k}_3(z,s) \end{pmatrix} = \sqrt{2s}\int_1^\infty \hat{I}(w,s)\,\mathrm{d}w,$$

where

$$\hat{I}(w,s) = \frac{1}{2\pi}\int_{-\infty+u_0 i}^{\infty+u_0 i} < \cdot > \mathrm{e}^{-sL\sqrt{b^2+u^2}w + siuz}\,\mathrm{d}u = \begin{pmatrix} \hat{I}_2 \\ \hat{I}_3 \end{pmatrix}. \tag{5.8}$$

It is hoped that the final Laplace inversion of k_2, k_3 on time can be done by inspection. By the use of Cagniard–de Hoop method and letting

$$L\sqrt{b^2+u^2}w - uzi = t \tag{5.9}$$

Eqn. (5.11) can be solved for u to yield

$$u_{L\pm} = \frac{tzi \pm wL\sqrt{t^2-(z^2+w^2L^2)b^2}}{z^2+w^2L^2}, \tag{5.10}$$

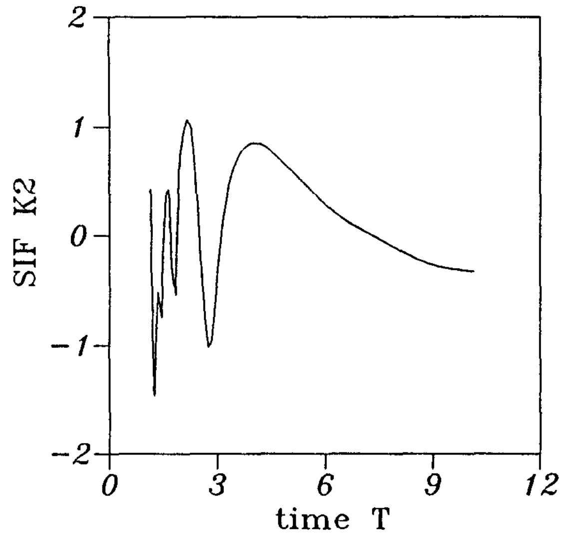

Fig. 3. The normalized stress intensity factor k_2 versus normalized time $C_s t/L$. When $P_1 = P_2 = 1.0$, $z = 0.4L$ and $T_0 = \sqrt{1.16}$.

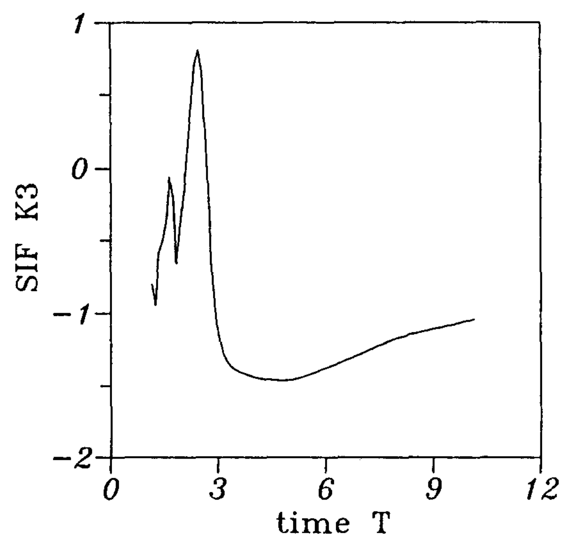

Fig. 4. The normalized stress intensity factor k_3 versus normalized time $C_s t/L$. When $P_1 = P_2 = 1.0$, $z = 0.4L$ and $T_0 = \sqrt{1.16}$.

where the positive square root is taken.

If $R_e(u_{L\pm}) = 0$, one has $t = b\sqrt{z^2 + w^2L^2}$, and the vertex of the hyperbola is thus defined by

$$u = \frac{tz}{z^2 + w^2L^2}i = \frac{zbi}{\sqrt{z^2 + w^2L^2}}.$$

The transition to the Cagniard-contour defined by $u_{L\pm}$ is very simple in this case because no poles and branch points are crossed. Along the Cagniard contour (Fig. 2) one now introduces

t as the new variable, which leads to

$$\hat{I}_2(w,s) = \frac{1}{\pi^2}\int_{b\cdot\sqrt{z^2+w^2L^2}}^{\infty}\left\langle R_e\left\{\frac{2u_{L+}(\sqrt{b^2+u_{L+}^2}+u_{L+})^2\sqrt[4]{b^2+u_{L+}^2}}{(\sqrt{b^2+u_{L+}^2}+u_{L+})^2+\frac{k}{b^2}(\sqrt{c^2+u_{L+}^2}+u_{L+})^2\cdot\tilde{S}_+^2}\right.\right.$$

$$\left.\times\frac{P_1\sqrt{b^2+u_{L+}^2}w-iP_2u_{L+}}{(b^2+u_{L+}^2)w^2-u_{L+}^2}\frac{(w-1)^{1/2}\frac{\partial u_{L+}}{\partial t}}{\left(\sqrt{\frac{c^2+u_{L+}^2}{b^2+u_{L+}^2}}-w\right)S_-(\sqrt{b^2+u_{L+}^2}w)}\right\}$$

$$-R_e\left\{\frac{2ku_{L+}}{b^2}\frac{\tilde{S}_+(u_{L+})}{\sqrt{w-1}}\frac{(\sqrt{b^2+u_{L+}^2}+u_{L+})\sqrt[4]{b^2+u_{L+}^2}(\sqrt{c^2+u_{L+}^2}+u_{L+})}{(\sqrt{b^2+u_{L+}^2}+u_{L+})^2+\frac{k}{b^2}(\sqrt{b^2+u_{L+}^2}+u_{L+})^2\tilde{S}_+^2}\right.$$

$$\left.\cdot\frac{-P_1u_{L+}+P_2i\sqrt{b^2+u_{L+}^2}w}{(b^2+u_{L+}^2)w^2-u_{L+}^2}\frac{\partial u_{L+}}{\partial t}\right\}$$

$$+R_e\cdot\left\{\frac{\sqrt[4]{b^2+u_{L+}^2}(w-1)^{1/2}\frac{\partial u_{L+}}{\partial t}}{(\sqrt{b^2+u_{L+}^2}w+u_{L+})\left(\sqrt{\frac{c^2+u_{L+}^2}{b^2+u_{L+}^2}}-w\right)}\right.$$

$$\left.\left.\times\frac{(P_1\sqrt{b^2+u_{L+}^2}w-iP_2u_{L+})}{S_-(\sqrt{b^2+u_{L+}^2}w)}\right\}\right\rangle e^{-st}\cdot dt, \tag{5.11}$$

$$\hat{I}_3(w,s) = \frac{1}{\pi^2}\int_{b\cdot\sqrt{z^2+w^2L^2}}^{\infty}\left\langle R_e\left\{-\frac{2u_{L+}i(\sqrt{b^2+u_{L+}^2}+u_{L+})(\sqrt{c^2+u_{L+}^2}+u_{L+})}{(\sqrt{b^2+u_{L+}^2}+u_{L+})^2+\frac{k}{b^2}(\sqrt{c^2+u_{L+}^2}+u_{L+})^2\cdot\tilde{S}_+^2}\right.\right.$$

$$\times\tilde{S}_+(u_{L+})\cdot\frac{\sqrt[4]{b^2+u_{L+}^2}(w-1)^{1/2}}{\left(\sqrt{\frac{c^2+u_{L+}^2}{b^2+u_{L+}^2}}-w\right)}$$

$$\left.\times\frac{(P_1\sqrt{b^2+u_{L+}^2}w-iP_2u_{L+})}{S_-(\sqrt{b^2+u_{L+}^2}w)((b^2+u_{L+}^2)w^2-u_{L+}^2)}\frac{\partial u_{L+}}{\partial t}\right\}$$

$$+R_e\left\{-\frac{2ku_{L+}}{b^2}\frac{(\sqrt{c^2+u_{L+}^2}+u_{L+})^2\tilde{S}_+^2\sqrt[4]{b^2+u_{L+}^2}}{(\sqrt{b^2+u_{L+}^2}+u_{L+})^2+\frac{k}{b^2}(\sqrt{c^2+u_{L+}^2}+u_{L+})^2\tilde{S}_+^2}\right.$$

$$\times \frac{P_1 i u_{L+} + P_2\sqrt{b^2+u_{L+}^2}\,w}{(w-1)^{1/2}} \frac{\partial u_{L+}}{\partial t} \frac{1}{(b^2+u_{L+}^2)w^2 - u_{L+}^2} \Bigg\}$$

$$+R_e\left\{-\frac{\sqrt[4]{b^2+u_{L+}^2}}{\sqrt{b^2+u_{L+}^2}\,w+u_{L+}} \frac{P_1 i u_{L+} + P_2\sqrt{b^2+u_{L+}^2}\,w}{(w-1)^{1/2}} \frac{\partial u_{L+}}{\partial t}\right\}\Bigg\rangle \mathrm{e}^{-st}\cdot \mathrm{d}t, \qquad (5.12)$$

the inverse Laplace transform of $\hat{I}$ may thus be expressed as

$$I(w,t) = \frac{1}{\pi^2}(\cdot)H(t - b\cdot\sqrt{z^2+w^2L^2}). \qquad (5.13)$$

In order that the convolution theorem for Laplace transform may be applied, one defines two functions H_2, H_3 as

$$\left.\begin{aligned} k_2(z,t) &= \frac{\partial H_2(z,t)}{\partial t} \quad H_2(z,0)=0 \\ k_2(z,t) &= \frac{\partial H_3(z,t)}{\partial t} \quad H_3(z,0)=0 \end{aligned}\right\}. \qquad (5.14)$$

Then

$$\left.\begin{aligned} \hat{k}_2(z,s) &= s\hat{H}_2(z,s) \\ \hat{k}_3(z,s) &= s\hat{H}_3(z,s) \end{aligned}\right\} \qquad (5.15)$$

which, coupled with (5.11), (5.12), (5.8), yields

$$\begin{pmatrix} \hat{H}_2(z,s) \\ \hat{H}_3(z,s) \end{pmatrix} = \sqrt{\frac{2}{s}} \int_1^{\infty} \hat{I}(w,s)\,\mathrm{d}w, \qquad (5.16)$$

thus

$$\begin{pmatrix} H_2(z,t) \\ H_3(z,t) \end{pmatrix} = \int_1^{\sqrt{\frac{t^2}{b^2L^2} - z^2/L^2}} \int_{\sqrt{z^2+w^2L^2}}^{t} I(w,\tau)\sqrt{\frac{2}{\pi(t-\tau)}}\,\mathrm{d}\tau\,\mathrm{d}w. \qquad (5.17)$$

By setting $T = t/bL, \hat{z} = z/L$, (5.17) can be rewritten as

$$\begin{aligned} H_2(\hat{z},T) &= \frac{\sqrt{2}b}{\pi^{5/2}L^{1/2}} \int_1^{\sqrt{T^2-\hat{z}^2}} \int_{\sqrt{\hat{z}^2+w^2}}^{T} I_2(w,\hat{\tau}) \frac{\mathrm{d}\hat{\tau}}{\sqrt{T-\hat{\tau}}}\,\mathrm{d}w, \\ H_3(\hat{z},T) &= \frac{\sqrt{2}b}{\pi^{5/2}L^{1/2}} \int_1^{\sqrt{T^2-\hat{z}^2}} \int_{\sqrt{\hat{z}^2+w^2}}^{T} I_3(w,\hat{\tau}) \frac{\mathrm{d}\hat{\tau}}{\sqrt{T-\hat{\tau}}}\,\mathrm{d}w. \end{aligned} \qquad (5.18)$$

Concluding from (5.18) and (5.14), one has

$$k_2(\hat{z},T) =$$

$$\frac{\sqrt{2}}{\pi^{5/2}L^{3/2}} \frac{\partial}{\partial T} \Bigg\langle \int_1^{\sqrt{T^2-\hat{z}^2}} \int_{\sqrt{\hat{z}^2+w^2}}^{T}$$

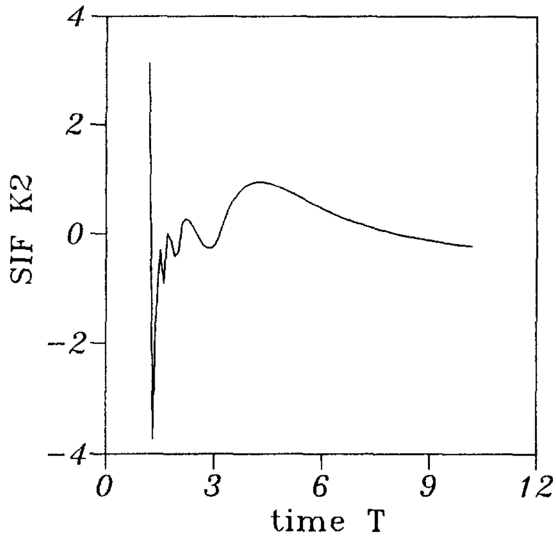

Fig. 5. The normalized stress intensity factor k_2 versus normalized time $C_s t/L$. When $P_1 = P_2 = 1.0$, $z = 0.6L$ and $T_0 = \sqrt{1.36}$.

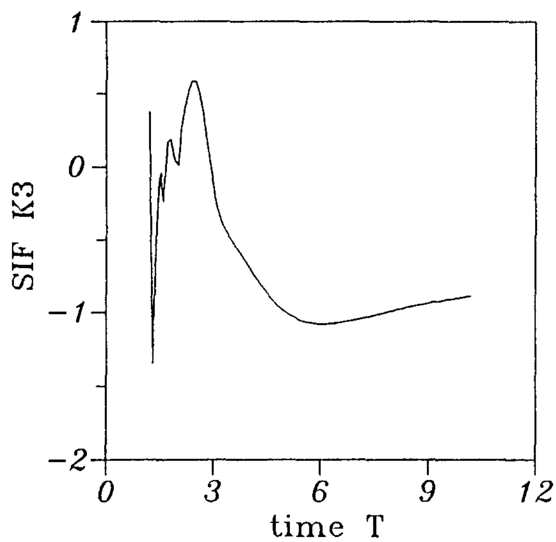

Fig. 6. The normalized stress intensity factor k_3 versus normalized time $C_s t/L$. When $P_1 = P_2 = 1.0$, $z = 0.6L$ and $T_0 = \sqrt{1.36}$.

$$\times \left\{ R_e \left\{ \frac{2\hat{u}_{L+}(\sqrt{1+\hat{u}_{L+}^2}+\hat{u}_{L+})^2 \sqrt[4]{1+\hat{u}_{L+}^2}}{(\sqrt{1+\hat{u}_{L+}^2}+\hat{u}_{L+})^2 + \frac{k}{b^2}(\sqrt{\hat{c}^2+\hat{u}_{L+}^2}+\hat{u}_{L+})^2 \hat{S}_+^2} \right.\right.$$

$$\times \frac{P_1\sqrt{1+\hat{u}_{L+}^2}w - iP_2\hat{u}_{L+}}{(1+\hat{u}_{L+}^2)w^2-\hat{u}_{L+}^2} \frac{(w-1)^{1/2}\frac{\partial \hat{u}_{L+}}{\partial \tau}}{\left(\sqrt{\frac{\hat{c}^2+\hat{u}_{L+}^2}{1+\hat{u}_{L+}^2}}-w\right)} \frac{1}{S_-(\sqrt{1+\hat{u}_{L+}^2}w)}\Bigg\}$$

$$-R_e\left\{\frac{2k\hat{u}_{L+}}{b^2}\frac{\hat{S}_+}{\sqrt{w-1}}\frac{(\sqrt{1+\hat{u}_{L+}^2}+\hat{u}_{L+})\sqrt[4]{1+\hat{u}_{L+}^2}(\sqrt{\hat{c}^2+\hat{u}_{L+}^2}+\hat{u}_{L+})}{(\sqrt{1+\hat{u}_{L+}^2}+\hat{u}_{L+})^2+\frac{k}{b^2}(\sqrt{1+\hat{u}_{L+}^2}+\hat{u}_{L+})^2\hat{S}_+^2}\right.$$

$$\left.\times \frac{-P_1\hat{u}_{L+}+P_2 i\sqrt{1+\hat{u}_{L+}^2}w}{(1+\hat{u}_{L+}^2)w^2-\hat{u}_{L+}^2}\frac{\partial \hat{u}_{L+}}{\partial \tau}\right\}$$

$$+R_e\left\{\frac{\sqrt[4]{1+\hat{u}_{L+}^2}(w-1)^{1/2}\frac{\partial u_{L+}}{\partial \tau}}{(\sqrt{1+\hat{u}_{L+}^2}w+\hat{u}_{L+})\left(\sqrt{\frac{\hat{c}^2+\hat{u}_{L+}^2}{1+\hat{u}_{L+}^2}}-w\right)}\right.$$

$$\left.\times \frac{(P_1\sqrt{1+\hat{u}_{L+}^2}w-iP_2\hat{u}_{L+})}{S_-(\sqrt{1+\hat{u}_{L+}^2}w)}\right\}\Bigg\}\frac{d\tau}{\sqrt{T-\tau}}dw\Bigg\rangle, \quad (5.19a)$$

$$k_3(\hat{z},T) =$$

$$\frac{\sqrt{2}}{\pi^{5/2}L^{3/2}}\frac{\partial}{\partial T}\left\langle \int_1^{\sqrt{T^2-\hat{z}^2}}\right.$$

$$\times \int_{\sqrt{\hat{z}^2+w^2}}^{T}\left\{R_e\left\{-\frac{2\hat{u}_{L+}i(\sqrt{1+\hat{u}_{L+}^2}+\hat{u}_{L+})(\sqrt{\hat{c}^2+\hat{u}_{L+}^2}+\hat{u}_{L+})}{(\sqrt{1+\hat{u}_{L+}^2}+\hat{u}_{L+})^2+\frac{k}{b^2}(\sqrt{\hat{c}^2+\hat{u}_{L+}^2}+\hat{u}_{L+})^2\hat{S}_+^2}\right.\right.$$

$$\times \hat{S}_+(\hat{u}_{L+})\frac{\sqrt[4]{1+\hat{u}_{L+}^2}(w-1)^{1/2}}{\left(\sqrt{\frac{\hat{c}^2+\hat{u}_{L+}^2}{1+\hat{u}_{L+}^2}}-w\right)}$$

$$\left.\times \frac{(P_1\sqrt{1+\hat{u}_{L+}^2}w-iP_2\hat{u}_{L+})}{S_-(\sqrt{1+\hat{u}_{L+}^2}w)((1+\hat{u}_{L+}^2)w^2-\hat{u}_{L+}^2)}\frac{\partial \hat{u}_{L+}}{\partial \tau}\right\}$$

$$+R_e\left\{-\frac{2k\hat{u}_{L+}}{b^2}\frac{(\sqrt{\hat{c}^2+\hat{u}_{L+}^2}+\hat{u}_{L+})^2\hat{S}_+^2\sqrt[4]{1+\hat{u}_{L+}^2}}{(\sqrt{1+\hat{u}_{L+}^2}+\hat{u}_{L+})^2+\frac{k}{b^2}(\sqrt{\hat{c}^2+\hat{u}_{L+}^2}+\hat{u}_{L+})^2\hat{S}_+^2}\right.$$

$$\left.\times \frac{P_1 i\hat{u}_{L+}+P_2\sqrt{1+\hat{u}_{L+}^2}w}{(w-1)^{1/2}}\frac{\partial \hat{u}_{L+}}{\partial \tau}\frac{1}{(1+\hat{u}_{L+}^2)w^2-\hat{u}_{L+}^2}\right\}$$

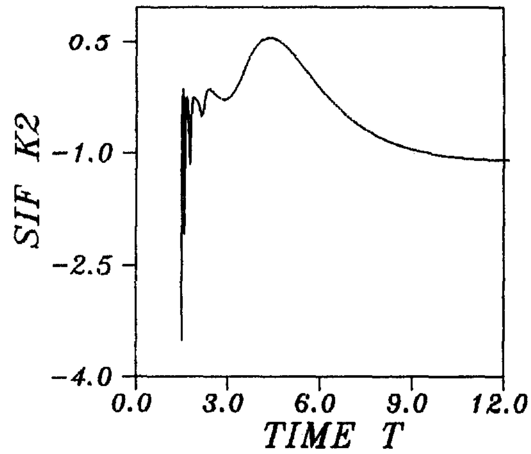

Fig. 7. The normalized stress intensity factor k_2 versus normalized time $C_s t/L$. When $P_1 = P_2 = 1.0$, $z = 0.8L$ and $T_0 = \sqrt{1.64}$.

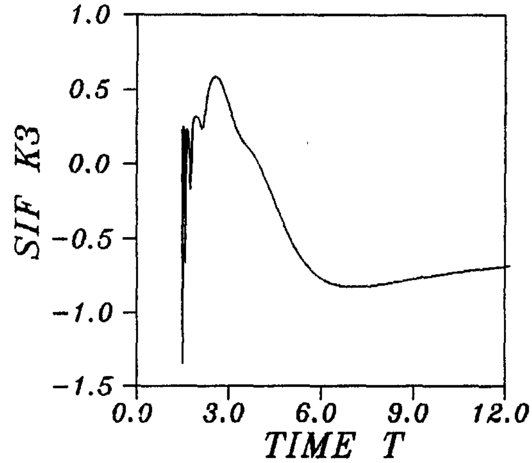

Fig. 8. The normalized stress intensity factor k_3 versus normalized time $C_s t/L$. When $P_1 = P_2 = 1.0$, $z = 0.8L$ and $T_0 = \sqrt{1.64}$.

$$+ R_e \left\{ - \frac{\sqrt[4]{1 + \hat{u}_{L+}^2}}{\sqrt{1 + \hat{u}_{L+}^2}\, w + \hat{u}_{L+}} \frac{P_1 i \hat{u}_{L+} + P_2 \sqrt{1 + \hat{u}_{L+}^2}\, w}{(w-1)^{1/2}} \frac{\partial \hat{u}_{L+}}{\partial \tau} \right\} \Bigg\}$$

$$\times \frac{\mathrm{d}\tau}{\sqrt{T - \tau}} \mathrm{d}w \Big\rangle, \tag{5.19b}$$

where

$$\hat{u}_{L+} = \frac{T\hat{z} + w\sqrt{T^2 - \hat{z}^2 - w^2}}{\hat{z}^2 + w^2}, \quad \hat{c} = \frac{c}{b}. \tag{5.19c}$$

6. Results and discussion

One useful check on the results obtained for $k_2(z,t), k_3(z,t)$ is that these results should be reduced to the stress intensity factor histories for the corresponding two-dimensional Lind

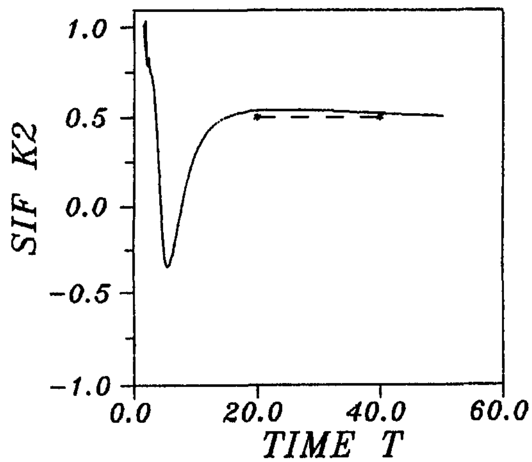

Fig. 9. The normalized stress intensity factor k_2 versus normalized time $C_s t/L$.When $P_1 = -1.0$, $P_2 = 0.0$, $z = L$ and $T_0 = \sqrt{2}$. — — — static SIF; — dynamic SIF.

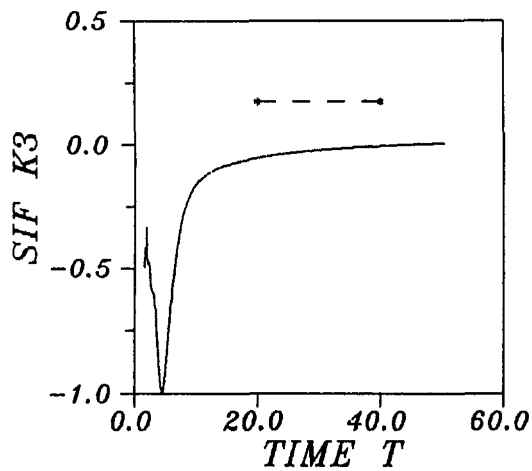

Fig. 10. The normalized stress intensity factor k_3 versus normalized time $C_s t/L$. When $P_1 = -1.0$, $P_2 = 0.0$, $z = L$ and $T_0 = \sqrt{2}$. — — — static SIF; — dynamic SIF.

load problem solved by Freund [2] when integrated over the range $-\infty < z < \infty$. If the integration is performed on (5.7), one has

$$\int_{-\infty}^{\infty} \begin{pmatrix} \hat{k}_2(z,s) \\ \hat{k}_3(z,s) \end{pmatrix} \mathrm{d}z = \sqrt{\frac{2}{s}\frac{1}{\pi}} \int_b^{\infty} \begin{pmatrix} \dfrac{-P_1(u-b)^{1/2}}{(u-c)s_-(u)} \\ -P_2/(u-b)^{1/2} \end{pmatrix} \mathrm{e}^{-sLu}\,\mathrm{d}u, \tag{6.1}$$

therefore

$$\int_{-\infty}^{\infty} \begin{pmatrix} k_2(z,t) \\ k_3(z,t) \end{pmatrix} \mathrm{d}z = \begin{pmatrix} \sqrt{\dfrac{2}{\pi l}} \displaystyle\int_b^{t/L} \frac{1}{\pi} \frac{P_1(\tau-b)^{1/2} d\tau}{(c-\tau)S_-(\tau)\sqrt{t/L-\tau}} \\ -\sqrt{\dfrac{2}{\pi L}} P_2 H(t - C_s L) \end{pmatrix}, \tag{6.2}$$

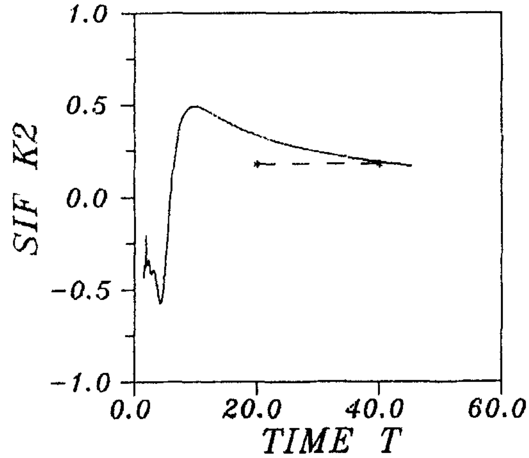

Fig. 11. The normalized stress intensity factor k_2 versus normalized time $C_s t/L$. When $P_1 = 0.0$, $P_2 = -1.0$, $z = L$ and $T_0 = \sqrt{2}$. – – – static SIF; — dynamic SIF.

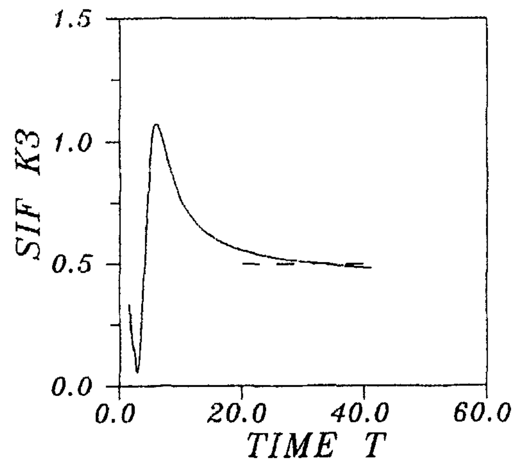

Fig. 12. The normalized stress intensity factor k_3 versus normalized time $C_s t/L$. When $P_1 = 0.0$, $P_2 = -1.0$, $z = L$ and $T_0 = \sqrt{2}$. – – – static SIF; — dynamic SIF.

which agree with the results presented in [2].

The integral in (5.19) has been evaluated numerically, the procedure of numerical calculation is that, firstly, $k_r(\hat{z}, T)(r = 2, 3)$ is written in the following form

$$k_r = \frac{1}{\pi}\frac{\partial}{\partial T}\left\langle \int_1^{\sqrt{T^2-\hat{z}^2}} \int_0^1 2\cdot\sqrt{T - \sqrt{\hat{z}^2 + w^2}} f_r(w, \tau(x))\, \mathrm{d}w\, \mathrm{d}x \right\rangle, \quad (r = 2, 3), \tag{6.3}$$

where

$$\tau(x) = \sqrt{\hat{z}^2 + w^2} + (T - \sqrt{\hat{z} + w^2})(1 - x^2), \tag{6.4}$$

then, the integrate calculation has been carried out by use of Gaussian quadrature formulas

$$k_r = \frac{1}{\pi}\sum_{i=1}^{N_1}\sum_{j=1}^{N_2}\left\{(d_1 d_2 + d_3 d_4) f_r(w_i, \tau_j) + d_2 d_3 \frac{\partial}{\partial T}[f_r(w_i, \tau_j)]\right\} Q_i R_j, \tag{6.5}$$

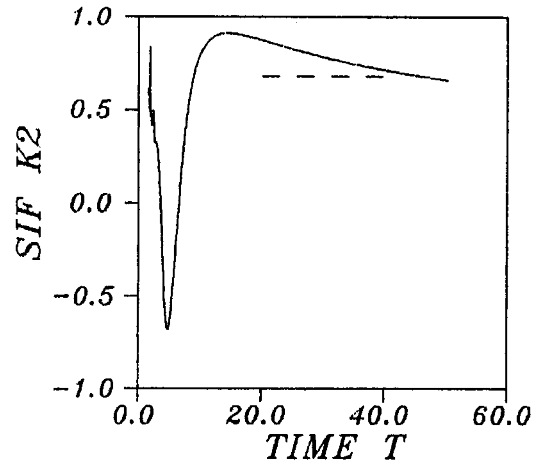

Fig. 13. The normalized stress intensity factor k_2 versus normalized time $C_s t/L$. When $P_1 = -1.0, P_2 = -1.0$, $z = L$ and $T_0 = \sqrt{2}$. – – – static SIF; — dynamic SIF.

where

$$\begin{aligned} w_i &= \frac{\sqrt{T^2 - \hat{z}^2} + 1}{2} + \frac{\sqrt{T^2 - \hat{z}^2} - 1}{2} y_i, \\ \tau_j &= \sqrt{\hat{z}^2 + w_i^2} + (T - \sqrt{\hat{z}^2 + w_i^2})(1 - x_j^2), \\ d_1 &= \frac{T}{2\sqrt{T^2 - \hat{z}^2}}, \\ d_2 &= \sqrt{T - \sqrt{\hat{z}^2 + w_i^2}}, \\ d_3 &= \frac{\sqrt{T^2 - \hat{z}^2} - 1}{2}, \\ d_4 &= \frac{1}{2d_2}(1 - \frac{w_i}{\sqrt{\hat{z}^2 + w_i^2}} d_1(1 + y_i)), \end{aligned} \qquad (6.6)$$

and

y_i is the ith zero of legendre polynomials $L_{N1}(x)$; x_j is the jth positive zero of legendre polynomials $L_{2N2}(x)$; Q_i is the Gaussian weights of order N_1; $R_j = 2W_j^{(2N_2)}$, $W_j^{(2N_2)}$ is the Gaussian weights of order $2N_2$.

In this paper, $N_1 = 12, N_2 = 10$ and the results of numerical evaluation for Poisson ratio $\nu = 0.3$ ($b = 1.87a$, $c = 2.02a$) are shown in Figs. 3–14. The time scale has been nondimensionalized so that T_0 corresponds to the arrival of the shear wave at the observation position z along the crack front. The dynamic stress intensity factors have been normalized by premultiplying (5.19) by $(\pi l)^{3/2}/\sqrt{2}$. Following the sudden application of the point loads, a point z along the crack edge is at rest until the arrival of the shear wave front.

At the observation position z near to the crack face, the transient field consists only of the plane wave parallel to the crack face and traveling away from it at speed C_s, and the shear loading does not generate a plane dilatational wave field, similar to the two dimensional situation [2].

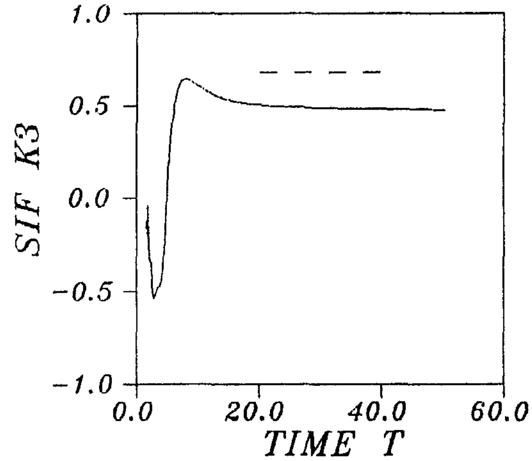

Fig. 14. The normalized stress intensity factor k_3 versus normalized time $C_s t/L$. When $P_1 = -1.0$, $P_2 = -1.0$, $z = L$ and $T_0 = \sqrt{2}$. – – – static SIF; — dynamic SIF.

After the arrival of the shear wave, attributed to the characteristic lengths in loading, the system of waves produced not only include the first arrival of the direct waves, but also the second reflection waves produced by the first waves interacting with crack edge. Because our solutions include a system of all waves' arrival at a fixed position at the same time, the results in Figs. 3–8 give us very complex and beautiful phenomena, similar to the mode I situations [9].

Figures 9–14 show the normalized stress intensity factors versus normalized time C_s/tL. From these figures we can observe that the transient stress intensity factor histories decay very gradually toward their equilibrium stress intensity factor distributions for this configuration. Here

$$K_2(\infty, z) = -\frac{\sqrt{2}P_1}{(\pi L)^{3/2}} \frac{1}{1+(z/L)^2}\left[1 + \frac{2\nu}{2-\nu}\frac{1-z^2/L^2}{1+z^2/L^2}\right]$$
$$-\frac{\sqrt{2}P_2}{(\pi L)^{3/2}}\frac{4\nu}{2-\nu}\frac{z/L}{(1+z^2/L^2)^2}$$
$$K_3(\infty, z) = -\frac{\sqrt{2}P_2}{(\pi L)^{3/2}} \frac{1}{1+(z/L)^2}\left[1 - \frac{2\nu}{2-\nu}\frac{1-z^2/L^2}{1+z^2/L^2}\right]$$
$$-\frac{\sqrt{2}P_1}{(\pi L)^{3/2}}\frac{4\nu}{2-\nu}\frac{z/L}{(1+z^2/L^2)^2}.$$

This completes the analysis of the three-dimensional stress intensity factor histories for the particular applied traction distribution (2.5). Results could be derived for a number of other traction distributions in a similar way.

APPENDIX

From (4.15), one has

$$G_+(\eta) = -\frac{1}{2\pi i}\int_{B_r} \frac{G(z) - G_0}{Z- \mid u \mid}\frac{\mathrm{d}z}{Z-\eta}, \qquad \text{(see Fig 2)}$$

$$= (\text{By Jodan lemma}) \int_{c_1} + \int_{c_2}$$

$$= \frac{1}{2\pi i} \int_{\sqrt{b^2+u^2}}^{\infty} \frac{\mathrm{d}t}{(t+|u|)(t+\eta)} \left\{ \begin{bmatrix} \frac{-i(-\sqrt{b^2+u^2}+t)^{1/2}(-P_1 t + iP_2 u)}{\sqrt{k}/b(\sqrt{c^2+u^2}-t)S_-(t,u)} \\ \frac{i}{(t-\sqrt{b^2+u^2})^{1/2}}(P_1 iu + P_2 t) \end{bmatrix} \mathrm{e}^{-sLt} - G_0 \right\}$$

$$- \frac{1}{2\pi i} \int_{\sqrt{b^2+u^2}}^{\infty} \frac{\mathrm{d}t}{(t+|u|)(t+\eta)} \left\{ \begin{bmatrix} \frac{i(-\sqrt{b^2+u^2}+t)^{1/2}(-P_1 t + iP_2 u)}{\sqrt{k}/b(\sqrt{c^2+u^2}-t)S_-(t,u)} \\ \frac{-i}{(t-\sqrt{b^2+u^2})^{1/2}}(P_1 iu + P_2 t) \end{bmatrix} \mathrm{e}^{-sLt} - G_0 \right\}$$

$$= \frac{-1}{\pi} \int_{\sqrt{b^2+u^2}}^{\infty} \frac{\mathrm{d}t}{(t+|u|)(t+\eta)} \left\{ \begin{bmatrix} \frac{(t-\sqrt{b^2+u^2})^{1/2}(P_1 t - iP_2 u)}{\sqrt{k}/b(\sqrt{c^2+u^2}-t)S_-(t,u)} \\ \frac{P_1 iu + P_2 t}{(t-\sqrt{b^2+u^2})^{1/2}} \end{bmatrix} \mathrm{e}^{-sLt} \right\}$$

Substituting for $G_+(\eta)$, in (5.4), one may obtain (5.5), (5.6).

Acknowledgements

This work was supported by the National Natural Science Foundation of China. Critical comments from two anonymous reviewers have led to substantial revision of the initial manuscript. We would like to express special thanks to each of them.

References

1. L.B. Freund, *Journal of the Mechanics and Physics of Solids* 20 (1972) 129–140.
2. L.B. Freund, *Dynamic Fracture Mechanics*, Cambridge University Press (1990).
3. J.D. Achenbach and A. Gautesen, *Journal of Applied Mechanics* 44 (1977) 243.
4. L.B. Freund, *Journal of the Mechanics and Physics of Solids* 35 (1987) 61–72.
5. J.C. Ramirez, *Quaterly of Applied Mathematics* XLV (1987) 361–376.
6. C.R. Champion, *International Journal of Solids and Structures* 24:3 (1988) 285–300.
7. M.K. Kuo and S.H. Cheng, *International Journal of Solids and Structures* 25:6 (1991) 751–768.
8. M.K. Kuo and T.Y. Chen, *Engineering Fracture Mechanics* 42:5 (1992) 805–813.
9. Li Xiang Ping and Liu Chun Tu, *Scientia Sinica A* 24:3 (1994) in Chinese.
10. J.D. Achenbach, A.K. Gautesen and H. McMaken, *Ray Method for Waves in Elastic Solids*, Boston (1982).